

Gas Accretion by Globular Clusters and Nucleated Dwarf Galaxies and the Formation of the Arches and Quintuplet Clusters.

Douglas N. C. Lin

University of California, Lick Observatory, Santa Cruz, CA 95064

& Stephen D. Murray

*University of California, Lawrence Livermore National Laboratory, P.O. Box 808,
Livermore, CA 94550*

ABSTRACT

We consider here the collective accretion of gas by globular clusters and dwarf galaxies moving through the interstellar medium. In the limit of high velocity and/or sound speed of the ISM, the collective potential of the cluster is insufficient to accrete significant amounts of gas, and stars within the systems accrete gas individually. We show, however, that when the sound speed or the relative velocity of the ambient medium is less than the central velocity dispersion of the cluster, it is accreted into the collective potential of the cluster prior to being accreted onto the individual stars within the cluster. The collective rate is strongly enhanced relative to the individual rates. This effect may potentially modify the white dwarf cooling sequence in globular clusters with low-inclination and low-eccentricity Galactic orbits, and lead to the rejuvenation of some marginally surviving cores of globular clusters and nucleated dwarf galaxies near the Galactic center. Such effects will only occur rarely, but may explain the existence of clusters of young, massive stars near the Galactic center.

Subject headings: galaxies: dwarf — galaxies: evolution — clusters: globular — clusters: open — hydrodynamics — methods: numerical

1. Introduction

Stars within individual open and globular clusters are coeval and have remarkably homogeneous chemical composition (see, eg. Penny & Dickens 1986; Richer & Fahlman 1986; Stetson & Harris 1988; Ferraro et al. 1991, 1992; Kraft et al. 1992; Langer et al. 1992;

Suntzeff 1993; Quillen 2002; Wilden et al. 2002). These properties provide strong constraints upon theories of star formation and evolution within these objects. In the most metal deficient globular clusters such as M92, the total heavy element content is comparable to the output of a small number of supernova events. The observed upper limit on the color spread among their giant branch stars implies their metallicity dispersion $\Delta Z < 10 - 20\%$. Such small spreads place limits on the accretion of enriched interstellar medium by the main sequence progenitors, which can be strengthened further using differential spectroscopy.

The accretion of the interstellar medium has more dramatic effects on both white dwarf and neutron stars. The white dwarf cooling sequences in both open and globular clusters are used as probes to determine the ages of these oldest stellar subsystems in the Milky Way galaxy (Richer et al. 1997, 1998; von Hippel & Gilmore 2000; Kalirai et al. 2001; Andreuzzi et al. 2002; Hansen et al. 2002). The intrinsic luminosity of the white dwarf is, however, typically $< 10^{-3}L_{\odot}$. Accretion of ambient gas at a rate $> 10^{-14}M_{\odot} \text{ yr}^{-1}$ would generate sufficient energy to modify both the color and magnitude of these degenerate dwarfs. Although the expected accretion rate of individual halo stars is several magnitudes below this value, it is not clear whether gas can be accreted first, at a sufficiently high rate, into the collective gravitational potential of individual clusters. The increased ambient density within the cluster would then enhance the accretion of the individual stars.

The accretion of ambient gas by moving bodies is a classical problem. Many studies have been focused on the flow around compact stars with a point mass potential (cf Frank, King & Raine 2002). Although clusters have much larger masses than individual stars, their potential is relatively shallow. In this paper we consider the efficiency of accretion in these cluster potentials. We are interested in determining the accretion rate for clusters with a range of velocities relative to the ambient medium. Cases with high relative velocity and sound speed represent globular clusters belonging to the halo and thick disk populations. Cases with low relative velocity and sound speed are more relevant to young open clusters, globular clusters that have sedimented into the galactic disk, and the residual dense cores of globular clusters or nucleated dwarf galaxies near the Galactic center.

In §2, we briefly recapitulate the relevant equations which describe the accretion flow. We deduce analytically a condition for the clusters to accrete gas collectively. Because the flow is multi-dimensional in nature, we adopt a numerical approach to verify our analytic approximation. We describe the numerical scheme and the range of model parameters and the results of these calculations in §3. These results are applied, in §4, to study the accretion of gas onto sedimented globular clusters as well as residual dense cores of clusters and nucleated dwarf galaxies near the Galactic center. In §5, we summarize our results and discuss their implications.

2. Accretion Onto a Shallow Potential

The basic governing equations for the ambient gas are the continuity and momentum equations. In order to highlight the dominant physical effects, we neglect the energy equation and adopt a polytropic equation of state. In general, the accretion flow onto a gravitating body is known to be unstable and unsteady. Because we are interested in the time-averaged accretion rates for illustration purpose, we seek steady state solutions of the governing equations such that

$$\nabla \cdot \rho \mathbf{u} = 0 \quad (1)$$

$$\rho \mathbf{u} \cdot \nabla \mathbf{u} = -\nabla P - \rho \nabla \phi \quad (2)$$

where ρ , P , and \mathbf{u} are the density, pressure, and velocity of the background gas. The gravitational potential of the cluster can be approximated with a Plummer potential,

$$\phi(R) = \frac{-GM_d}{(R_c^2 + R^2)^{1/2}}, \quad (3)$$

where M_d is the total gravitating mass, R_c is the core radius, inside of which the density of the gravitating matter is approximately constant, and R is the distance from the center of the potential. The Plummer potential is relatively centrally concentrated, and has been used to model globular clusters (Plummer 1911).

Equations (1) and (2) are multi-dimensional in nature, and they are treated numerically in the next section. We can, however, obtain some approximate analytic solutions to delineate various regimes of interest. With a polytropic equation of state, in which $P = K\rho^\gamma$ where K and γ are the adiabatic constant and the polytropic power index, we find from equations (2) and (3) that

$$\tilde{\mathbf{u}} \cdot \nabla \tilde{\mathbf{u}} = -\tilde{c}_s^2 \nabla \ln \rho - \xi(1 + \xi^2)^{-3/2} \nabla \xi \quad (4)$$

where

$$\xi = R/R_c \quad (5)$$

is a dimensionless radius. The quantities $\tilde{\mathbf{u}}$ and \tilde{c}_s are dimensionless speeds, defined as

$$\tilde{\mathbf{u}} = \frac{\mathbf{u}}{(GM_d/R_c)^{1/2}}, \quad (6)$$

and

$$\tilde{c}_s = \frac{C_s}{(GM_d/R_c)^{1/2}}, \quad (7)$$

where C_s is the sound speed of the fluid. From the continuity equation (1),

$$\tilde{\mathbf{u}} \cdot \nabla \ln \rho = \nabla \cdot \tilde{\mathbf{u}}. \quad (8)$$

We now consider three limiting cases. We first consider the possibility of very small R_c such that both $\tilde{u}(\xi = \infty) \equiv \tilde{u}_\infty \ll 1$ and $\tilde{c}_s(\xi = \infty) \equiv \tilde{c}_\infty \ll 1$. In this limit, the potential essentially reduces to that of a point mass and the accretion rate is given by Bondi solution (Bondi 1952; Hoyle & Lyttleton 1941; Shu 1992), such that

$$\dot{M}_c = A(\gamma)\pi\rho(\infty)(C_\infty^2 + u_\infty^2)^{1/2}R_B^2 \quad (9)$$

where A is a constant of order unity, C_∞ and u_∞ are, respectively, the non-normalized sound speed and flow velocity. The Bondi radius is given by

$$R_B = \frac{GM_d}{(C_\infty^2 + u_\infty^2)}, \quad (10)$$

so that

$$\dot{M}_c = A(\gamma)10^{25} \left(\frac{n_\infty}{10^2 \text{ cm}^{-3}} \right) \left(\frac{M_d}{10^6 M_\odot} \right)^2 \left(1 + \frac{C_\infty^2}{u_\infty^2} \right)^{-3/2} \left(\frac{u_\infty}{10 \text{ km s}^{-1}} \right)^{-3} \text{ g s}^{-1} \quad (11)$$

where $n_\infty = \rho_\infty/m_h$ and m_h is the mass of the hydrogen atom.

We note that the above form of R_B is derived for a point-mass potential, and so is only a good approximation for our models when R_B significantly exceeds R_c . We now consider two limiting cases with finite values of R_c . In case 2, we consider $\tilde{c}_s(\infty) \gg \tilde{u}(\infty)$, such that the flow is nearly spherically symmetric and equations(4) and (8) reduce to

$$\frac{d\ln\tilde{u}}{d\ln\xi} = \left(\frac{1}{\tilde{u}^2 - \tilde{c}_s^2} \right) \left(2\tilde{c}_s^2 - \frac{\xi^2}{(1 + \xi^2)^{3/2}} \right). \quad (12)$$

The maximum value of $\xi^2/(1 + \xi^2)^{3/2}$ occurs at $\xi = \xi_m \equiv \sqrt{2}$. Because \tilde{c}_s is a monotonically decreasing function of ξ , the numerator of the right side of equation (12) remains positive definite provided

$$C_s(\infty) > 3^{-3/4}(GM_d/R_c)^{1/2}. \quad (13)$$

Consequently, $|\tilde{u}| < \tilde{c}_s$ throughout the flow. The ambient gas therefore collects into a quasi-static atmosphere, with a density distribution given by

$$\rho(R) = \left[\rho_\infty^{\gamma-1} + \left(\frac{\gamma-1}{K\gamma} \right) \frac{GM_d}{(R^2 + R_c^2)^{1/2}} \right]^{1/(\gamma-1)} = \rho_\infty \left[1 + \frac{\gamma-1}{\tilde{c}_s^2(\infty)(1 + \xi^2)^{1/2}} \right]^{1/(\gamma-1)} \quad (14)$$

where ρ_∞ is the density of the ambient medium. If $C_\infty = C_s(\infty) > (GM_d/R_c)^{1/2}$, the density enhancement throughout the cluster is very small.

The relative motion of typical globular clusters with respect to the interstellar medium is generally supersonic, *i.e.* $\tilde{c}_\infty \ll u_\infty$. The flow pattern for passage around the cluster with

a large relative velocity, u_∞ , is multi-dimensional and complex. In line with the conventional treatment of Bondi-Hoyle accretion flow, it is intuitively tempting to modify the transition condition to be

$$C_\infty^2 + u_\infty^2 > GM_d/R_c. \quad (15)$$

When this condition is satisfied, it is more appropriate to use the Bondi-Hoyle accretion formula for individual stars

$$\begin{aligned} \dot{M}_* &= B(\gamma)\pi\rho(R)(GM_*)^2(C_\infty^2 + u_\infty^2)^{-3/2} \\ &= 10^{11} B(\gamma) \left(\frac{n_\infty}{10^2 \text{ cm}^{-3}}\right) \left(\frac{M_*}{M_\odot}\right)^2 \left(1 + \frac{C_\infty^2}{u_\infty^2}\right)^{-3/2} \left(\frac{u_\infty}{10 \text{ km s}^{-1}}\right)^{-3} \text{ g s}^{-1} \end{aligned} \quad (16)$$

where $B(\gamma)$ is a constant of order unity (it is not the same as A due to the difference in the potential) and M_* is the mass of the star. The total accretion rate of the cluster is

$$\dot{M}_t = N\dot{M}_* \quad (17)$$

where the number of stars in the cluster is $N \sim M_d/M_*$. But when equation (15) is not satisfied, \dot{M}_c in equation (9) is the more appropriate rate for the cluster. Note that

$$\dot{M}_c \sim N\dot{M}_t \gg \dot{M}_t. \quad (18)$$

This inequality clearly demonstrate that the collective effect of the cluster would be greater than sum of the individual stellar contributions if the it moves subsonically through the interstellar medium.

In the next section, we will carry out 3-D numerical computations to verify the condition in equation (15). Here we provide some analytic approximation for the limit that $u_\infty \gg C_\infty$. Without the loss of generality, we consider a case 3 in which the ambient gas is approaching a cluster in the x direction and the downstream flow velocities can be written as $u_x = u_\infty + \delta u_x$ and $u_y = \delta u_y$. Neglecting contribution from the pressure term in equation (4), we find that along the streamline with an initial impact distant R_i ,

$$\frac{\delta u_x}{u_\infty} \simeq -\frac{GM_d}{u_\infty^2(R_i^2 + R_c^2)^{1/2}}. \quad (19)$$

In the absence of shock dissipation, the potential vorticity, ω/ρ , and the Bernoulli energy, $|u|^2/2 + W + \phi$, are constant of motion along stream lines. In the limit that the enthalpy $W = \int dP/\rho$ is small compared with the kinetic and potential energy, the Bernoulli constant implies that $|\delta u_y/u_\infty| \sim |\delta u_x/u_\infty|$. The deflection angle of the stream line $\delta y_u/u_\infty$ is small in the limit $u_\infty^2 > GM_d/R_c$. We also note, from the conservation of the potential vorticity, that, in the high velocity limit, the modification of ρ is small despite the slight convergence of the streamlines.

3. Numerical Models

3.1. Method

The above analytic approximation is greatly simplified. The flow is actually multidimensional in nature. We therefore proceed by considering multidimensional simulations of accretion by a defined potential moving relative to a dense gas cloud. The results found here shall be used to validate the analytic estimates of § 2.

The numerical code we use is Cosmos. It is a massively parallel, multidimensional, radiation-chemo-hydrodynamics finite difference code developed at Lawrence Livermore National Laboratory. This scheme, and tests of the code are described in Anninos & Fragile (2003), and Anninos, Fragile & Murray (2003). It has also been used to study the evolution of supernova-enriched material in dwarf galaxies by Fragile et al. (2003), and to study Roche Lobe overflow from cluster and galactic potentials by Murray, Dong & Lin (2003). The reader is referred to those papers for more details on Cosmos. We discuss here the settings used for the current work.

For a spherically symmetric potential, the unperturbed flow would be expected to be two-dimensional. In flows where $u_\infty \sim C_\infty$, however, an axisymmetric flow pattern may be unstable (Landau & Lifshitz 1959; Batchelor 1967). Our objective is to determine the time averaged accretion rate rather than to identify any flow instability. Because Cosmos is written in Cartesian coordinates, however, we cannot impose cylindrical symmetry upon the problem, and so the simulations are carried out in three-dimensions. So as to reduce computational expense, the models are quadrants, with one-fourth of the regions included.

We wish to examine the ability of a potential to accrete gas as a function of the relative speed of the potential through the gas, and the gas temperature. To improve the controlled nature of the models, we do not include radiative heating or cooling. The gas, instead, evolves adiabatically. The effects of radiative equilibrium are approximated by having the gas evolve with an adiabatic constant $\gamma = 1.01$, giving approximately isothermal behavior. In cases where sufficient gas is accreted for it to become self-shielded, cooling could decrease the temperature of the gas significantly, potentially enhancing the accretion rate beyond the values computed here.

Rather than examine the motion of a potential through a static cloud, we take the simpler, equivalent approach of viewing the encounter within the frame of the cluster, in which a dense cloud of gas sweeps over the fixed potential. The model clouds are extremely simple. They are slabs, with thickness $l = 100$ pc, moving across the problem with speeds of u_∞ .

As discussed in § 2, the important quantities are the relative speed of the cloud and the potential, u_∞ , and the sound speed of the gas, C_s , and these quantities are varied between the models. The gas within the dense slab has temperature selected to give the desired value of C_s and a density chosen to cause it to be in pressure equilibrium with a hot background gas. The hot background gas in the problem has $T = 10^6$ K and $\rho = 1.6 \times 10^{-25}$ g cm $^{-3}$. The pressure of the gas, $nT = 10^5$, is chosen to be comparable to that expected within the central regions of galaxies, or in dense cooling flows.

As stated above, accretion by a potential moving relative to a gas cloud is complex. In the frame of the potential, the gas streamlines are bent towards the cluster center. Some shall intersect the center, while others converge along a line behind it. The convergence speed of the gas determines the reduction in its velocity relative to the potential due to shocks, and therefore whether or not the gas is accreted. In order to ensure that we are accurately measuring the mass of accreted gas, we carry out our models until the dense slab of gas has completely swept past the potential. The increase in the amount of gas within the potential radius as compared to that present initially, M_{acc} , is computed, and listed for each of our models. If the value of M_{acc} is seen to be changing at the end of the simulation, the model is run for additional time. The minimum time for the simulations is a few times $l/u_\infty \approx 100\text{Myr} \left(\frac{u_\infty}{1\text{km/s}} \right)$.

For the models examined here, the total gravitating mass, $M_d = 7 \times 10^5 M_\odot$, and the core radius of the potential, $R_c = 10$ pc. To approximate the effects of external gravitational fields, the potential is flattened (the gravitational force goes to zero) beyond an assumed tidal radius $R_t = 80$ pc. The central velocity dispersion $\sigma = (GM_d/R_c)^{1/2} = 16$ km s $^{-1}$, similar to the values within many globular clusters (Pryor & Meylan 1993; Djorgovski 1993). In some centrally condensed clusters such as M15, σ can reach 20 km s $^{-1}$. In some nucleated dwarf galaxies, $\sigma > 30$ km s $^{-1}$ (Peterson & Caldwell 1993; Geha, Guhathakurta, & van der Marel 2002). In contrast, σ in the Pleiades and Hyades clusters are 0.6 and 0.2 – 0.4 km s $^{-1}$, respectively (Perryman et al. 1998; Chen & Zhao 1999; Madsen, Dravins, & Lindegren 2002). Despite these differences, the discussion in the previous section indicate that the governing equations can be normalized with dimensionless parameters and the results obtained therefrom can be scaled to the appropriate limits.

Self-gravity of the gas is not included in the models. This approximation should be adequate for most of our models, for which the accreted mass is less than the mass responsible for the potential. For two of the models discussed below, the accreted mass exceeds that of the potential. For those models, the inclusion of self-gravity would further enhance the accretion rate. Both because of this, and the additional cooling discussed above, the accreted masses for those two models should be treated as lower limits.

The physical dimensions of the models are 400x200x200 pc, with resolutions of 2 pc. The core radius, R_c , is therefore resolved by only 5 zones. While not highly resolved, the fraction of the accreted mass contained within the core is generally small, and so the limited resolution within the cores does not affect our conclusions.

3.2. Model Results

The parameters of the models which we have run are shown in Table 1. In the table are listed, for each model, the speed of the gas relative to the potential, u_∞ , the sound speed of the gas, C_s , the Bondi radius (as defined in equation 10), R_B , the crossing time of the potential across the dense slab at u_∞ , $\tau_c \equiv l/u_\infty$, the sound crossing time across R_B , $\tau_s \equiv R_B/C_s$, the amount of gas predicted by approximate theory to be accreted (see below), M_p , and the actual amount of gas accreted in the model, M_{acc} . The value of M_{acc} is taken as the increase in mass contained within R_B relative to that present at the beginning of the simulation, and we ensure that the value is not changing by the end of the simulation (see above).

The parameters of the models are chosen so as to span the range of possible behaviors. In Model 1, $u_\infty > \sigma$, while in Model 6, $C_s > \sigma$. In both models, little accretion is expected, but in Model 1 this is because of the high relative velocity, while in Model 6 it is due to the high sound speed of the gas. In Model 2, $u_\infty \approx \sigma \gg C_s$, while in Model 5, $C_s \approx \sigma \gg u_\infty$. Both models represent marginal conditions for accretion, but again for different reasons. In Model 3, $u_\infty = C_s \ll \sigma$, and so that model is expected to represent an ideal situation for substantial accretion. In Model 4, $u_\infty = C_s \approx \sigma$, and so, again, that model represents a marginal situation for accretion.

Snapshots showing the evolution of Model 2 are shown in Figure 1. In the figure, the dense slab of gas can be seen sweeping over the gravitational potential, which is visible due to its effect upon the density of the gas moving past it. Because $u_\infty \approx \phi^{\frac{1}{2}}$, some gas is pulled ahead of the cloud by the potential, and a large fraction of the gas within the tidal radius of the potential is accreted during the cloud passage. Once the dense slab of gas is past the potential, a small, dense core of accreted gas remains in the center of the potential. In the models which accrete significant amounts of gas, therefore, the gas rapidly evolves to a condensed configuration, such as is likely to lead to cooling of the gas, and greatly enhanced accretion by the individual stars within the system.

We may make a crude analytical estimate of the accreted mass if we assume that the potential acts as a “cookie cutter,” and that gas closer to the center of the potential than

R_B is accreted during the passage of the potential through the dense slab. The amount of gas that would be predicted to be accreted is then given by

$$M_p = \pi l R_B^2 \rho_s, \quad (20)$$

where ρ_s is the density of the gas in the slab. The calculated values of M_p are shown in Table 1.

As can be seen from the table, the values of M_{acc} and M_p are in fair agreement for some models, but not others. As indicated in §2, the expression of R_B in equation (10) is derived for a point-mass potential, and so is only a good approximation for our models when R_B significantly exceeds R_c , a condition violated in Models 1 and 6. For those models, the Bondi radius computed assuming a point mass potential lies within the core, where the Plummer potential actually flattens out. The true potential therefore never becomes as deep as required for substantial accretion, and $M_{acc} \ll M_p$. Because $u_\infty > C_s$ in Model 1, equation (17) is more appropriate to represent the gas accretion. We could not, however, include the fine grain structure of the potential due to individual stars in our simulations.

In the case of Model 3, $R_B > R_t$. Beyond R_t , the gravity of the potential can have no direct effect upon the gas, and so Equation 20 represents an overestimate of the amount of gas that is expected to be accreted. Had we used R_t instead of R_B in calculating the fiducial value of M_p , we would have found $M_p = 5.6 \times 10^7 M_\odot$, much closer to the value found for M_{acc} .

For the remaining models, $M_{acc} > M_p$. That discrepancy is likely to be the result of the simplistic assumption made in deriving M_p , that no hydrodynamic motion beyond R_t results from the accretion. That assumption is equivalent to assuming that $\tau_s > \tau_c$. In fact, for most of the models, τ_s is at least comparable to, and often substantially smaller than τ_c , indicating that the gas within the dense slab shall have time to undergo significant adjustments to a new hydrostatic equilibrium in response to the accretion. As gas is accreted by the potential, therefore, the resulting pressure gradient drives gas inward from beyond R_t , increasing the effective radius from which gas may be accreted. The resulting enhancement in the accretion causes $M_{acc} > M_p$, even for Model 6, for which $R_B < R_c$.

The results of these models indicate that the results of Section 2 represent reasonable estimates of the accretion rates onto cluster potentials, and that the ratio $(C_s^2 + u_\infty^2) / (GM_d/R)$ is crucial to determining the importance of accretion by the global potential. The greatest differences between the analytic and numerical results occur at low values of \dot{M} , where the accretion is insignificant.

4. Astrophysical Applications

We now consider three scenarios in which accretion may affect the evolution of stellar clusters. These include potential effects upon the metallicity dispersion and white dwarf cooling sequences of globular clusters, the stellar populations of clusters in the Galactic disk, and the rejuvenation of old clusters near the Galactic center.

4.1. Metallicity Dispersion and White Dwarf Sequence in Globular Clusters

Typical globular clusters in the Galactic halo have relatively high orbital inclination and eccentricity. In contrast, the interstellar medium consists of either warm (10^2 K) atomic or cold (10 K) molecular gas on nearly coplanar, circular Galactic orbits. The relative velocity of the halo clusters to the interstellar medium is in the range of 100 km s^{-1} . For these clusters, the collective effect of their potential is clearly insignificant, and cluster stars accrete as individual entities.

Scaling with an average number density of 10^2 cm^{-3} for atomic clouds, we find from equation (16) that $\dot{M}_* \sim 10^9 \text{ g s}^{-1}$. Over the age of the Galaxy, the total amount of mass accreted is $\sim 10^{-6} M_\odot$. Even for the most metal-deficient ($[\text{Fe}/\text{H}] \simeq -4$) stars known, the acquisition of this amount of interstellar gas, with a solar metallicity, would modify the metallicity of the star by less than 1%. Variations in Lithium abundance have been observed among subgiants in halo globular clusters (Deliyannis, Boesgaard, & King 1995; Castilho et al. 2000). Main sequence evolution almost certainly has depleted all the Lithium in the envelopes of globular clusters' main sequence stars and the above estimate for the accretion rate is too small to account for the observed data. But, Lithium is produced in the core through hot bottom burning and dredged up to the surface of stars on the asymptotic and red giant branches (Cameron & Fowler 1971; Sackmann, Smith, & Despain 1974; Sackmann & Boothroyd 1992). The consumption of a Jupiter-mass gas planet has also been suggested as a mechanism to replenish the surface Lithium content (Laws & Gonzalez 2001; Sandquist et al. 2002), though the depletion time scale for Lithium is relatively short.

For white dwarf stars, accretion at the above rate would lead to the release of energy at a rate $L_a \sim 10^{-7} L_\odot$, which is much smaller than that expected from the cooling of the oldest Galactic white dwarfs (Hansen 1999). Thus the accretion from the interstellar medium needs not be taken into account in the determination of the white dwarf cooling sequence.

In order, therefore, for accretion to have a significant effect upon either the metallicity of cluster stars, or upon the color and luminosity of white dwarfs, u_∞ must be reduced to $\sim 10 \text{ km s}^{-1}$, in which limit the effects of collective accretion by the overall cluster potential

would become important.

4.2. Sedimentation of Clusters into Galactic Disks

Although u_∞ for typical halo clusters is too large for them to accrete any significant amount of matter, their orbital properties may evolve. As halo clusters pass through the Galactic disk with a speed u_g , the wake of disk stars induce a drag force (dynamical friction), given by

$$F_d = 4C_d\pi G^2 M_d^2 \rho_d u_g^{-2} \quad (21)$$

where ρ_d is the stellar density in the galactic disk, the drag coefficient,

$$C_d = \ln\Lambda \left[\operatorname{erf}(X) - \frac{2X}{\pi^{1/2}} e^{-X^2} \right], \quad (22)$$

where $\Lambda = b_{\max}/R_c$, $X = u_g/(\sqrt{2}\sigma)$, and b_{\max} is the maximum effective impact parameter, which can be taken to be the density scale height H_d of the Galactic disk (Chandrasekhar 1943; Binney & Tremaine 1987). Because gas and stars are concentrated near the midplane, the rate of dissipation of the cluster's orbital energy, averaged over its Galactic orbital period, P_g , is

$$\dot{E} = 2 \left(\frac{F_d}{M_d} \right) \left(\frac{H_g}{u_z} \right) \left(\frac{u_g}{P_g} \right) \quad (23)$$

where $E = u_g^2/2$ is the kinetic energy relative to the disk and u_z is the velocity normal to the galactic disk. Clusters which cross the Galactic disk with large velocities would sediment into low inclination and low eccentricity orbits on a time scale $u_g^2/4\dot{E}$ (Artymowicz, Lin & Wampller 1993). Over a time interval, ΔT , the critical condition for clusters to attain small u_g and u_z , and therefore u_∞ is

$$\left(\frac{u_g}{V_c} \right)^3 \frac{u_z}{V_c} < 32C_d\pi G^2 \frac{M_d \Sigma_d}{M_g(a)^2} \frac{\Delta T}{P_g} \quad (24)$$

where the Galactic circular velocity $V_c = [GM_g(a)/a]^{1/2}$ at a radius a is determined by the Galactic mass $M_g(a)$ contained within it, and $\Sigma_d = \rho_d H_d$ is the surface density of the disk stars. For $V_c = 220 \text{ km s}^{-1}$ at $a = 10 \text{ kpc}$, equation (24) implies that clusters with $u_g \sim u_z < 0.3V_c$ or $u_g = V_c$ and $u_z < 10^{-2}V_c$ would sediment into the disk within the life span of the Galaxy. Because ΔT is a decreasing function of u_z and u_g , the inclination and eccentricity of the clusters' Galactic orbits quickly vanish, leading to a small u_∞ .

Based on the present phase-space distribution of globular clusters, several authors (Fall & Rees 1977; Keenan 1979; Ostriker & Gnedin 1997; Vesperini, 1998; van den Bosch et al.

1999; Hideaki & Yoshiaki 2003) have suggested that dynamical friction may have caused clusters with small initial orbital radii to undergo significant orbital evolution. There also exist clusters in a thick disk population, which have smaller values of u_∞ than typical halo clusters.

For clusters that are not on orbits highly inclined to the disk, collective accretion may become a significant factor in their evolution. As u_∞ is reduced to $\sim 10 \text{ km s}^{-1}$, \dot{M}_* approaches to 10^{13} g s^{-1} . More importantly, $u_\infty < (GM_d/R_c)^{1/2}$, and \dot{M}_c approaches 10^{25} g s^{-1} . The gas density ρ_c within the clusters' potential would increase until

$$\dot{M}_* \sim (M_d/M_*)\dot{M}_c \sim 10^{-7}(M_*/M_\odot)^2 M_\odot \text{ yr}^{-1}. \quad (25)$$

Because clusters have nearly isothermal stellar distribution function, u_∞ relative to the gas in the cluster is comparable to σ , and $\rho_c \sim (M_d/M_*)\rho_g \sim 10^{-16} \text{ g cm}^{-3}$. Gas within these clusters would achieve high densities.

Within this environment, the cluster stars would accrete gas and gain significant mass. Within one Galactic orbit, the observed metallicity of the stars could attain the solar value present in the interstellar medium. Gas accumulating within the core of the cluster potential may also trigger new star formation. With high temperatures and densities, the initial mass function may be heavily skewed toward the high-mass range (McKee & Tan 2003). As star formation proceeds, negative feedback from processes such as photoionization, stellar winds, and supernovae can modify the gas concentration, and terminate star formation (Dong, Lin, & Murray 2003). These negative feedback effects cannot, however, prevent re-accumulation of gas around the sedimented clusters after the newly formed massive stars evolve off the main sequence. The distinguishing properties of these sedimented clusters from open clusters are their centralized cores and rich population of white dwarfs, despite their gas rich environment and the pre-main-sequence color magnitude diagram.

There are no stellar clusters observed in the Galactic disk which bear these anticipated properties, as would be expected given the relatively small region of phase space occupied by clusters whose orbits would be heavily modified by dynamical friction. At early epochs, however, many more such clusters would be expected, as a natural extrapolation of the cold dark matter scenario in which merger events and the subsequent dynamical friction would lead to the dynamical evolution of not only globular clusters but also the cores of dwarf galaxies (Moore et al. 1999; Klypin et al. 1999; Metcalf 2002; Metcalf & Zhao 2002; Murray et al. 2003). Star formation via accretion onto stellar and dark matter potentials may therefore have played an important role in the early evolution of galaxies.

Accretion at lower levels than the maximum estimated above would still affect the white dwarf cooling sequences of clusters. Clusters with orbits on small radii, and close to the

galactic plane might therefore be expected to have white dwarf cooling sequences brighter than expected for their ages.

4.3. Accretion Onto Remnant Cores of Globular Clusters and Nucleated Dwarf Galaxies

Near the Galactic center, several young massive star clusters have been recently discovered (Nagata et al. 1990, 1995; Okuda et al. 1990; Figer et al. 1999). Besides their age, these clusters are unusual in that 1) the initial mass function of stars within them is highly skewed to the high mass range (Figer et al. 2002; Stolte et al. 2002); and 2) they have short dynamical life expectancy (Kim, Morris, & Lee 1999; Kim et al. 2000; Portegies Zwart, McMillan, & Gerhard 2003; MacMillan & Portegies Zwart 2003). One cluster, the Arches Cluster, contains up to $7 \times 10^4 M_{\odot}$ within a radius of 0.23 pc, and has a velocity dispersion of up to 22 km s^{-1} (Figer et al. 2002). In addition, the Quintuplet Cluster, the cluster around the Galactic center itself, and several other candidate clusters (Law & Yusef-Zadeh 2004) contain x-ray point sources. The presence of clusters of young, short-lived stars near the Galactic center is remarkable, given that it is an environment that is extremely hostile to the formation of star clusters.

Assuming that the above objects are all young and short-lived clusters, and that there is nothing unusual about the current epoch, then more than 10^4 such clusters would be expected to have existed over in the lifetime of the Galaxy. The inferred heavy element generation by the prolific production of massive stars would enrich the Galactic center region to well above the present level, unless gas is effectively removed from that region (cf Figer et al. 2004).

Based on the results of the current work, we suggest an alternative scenario for the origin of these extraordinary clusters. Under the influence of dynamical friction, globular clusters undergo orbital decay towards the Galactic center. As discussed above, dynamical friction is not important to the evolution of most clusters. It is computed, however, to have a significant effect for clusters within a few kpc of the Galactic center (e.g. Fall & Rees 1977). The evolution of such clusters, and accretion of gas by them, may explain the existence of young clusters of massive stars near the Galactic center.

During the course of the clusters' orbital decay, the Galactic tidal field gradually increases and their tidal radius gradually shrinks. Stars close to or outside of the tidal radius become detached while those near the dense core are retained (Oh & Lin 1992; Oh, Lin, & Aarseth 1995). Stellar loss also shortens the two-body relaxation time scale, enhances the central concentration, and shortens the tidal disruption time scale (Kim & Morris 2003).

With a core density comparable to that of post-collapse clusters M15 (Guhathakurta et al. 1996) and M30 (Yanny et al. 1994), systems with more than 10^4 stars can persist and be tidally preserved near the present location of Galactic center clusters. Less centrally dense clusters such as M13 (Cohen et al. 1997) are likely to be disrupted by the Galactic tide outside 30 pc.

We suggest that Arches and Quintuplet clusters are the rejuvenated cores of old globular clusters, which have retained their integrity as their orbits decay to the vicinity of the Galactic center. Of those, however, only a fraction have velocities relative to the atomic and molecular clouds that are sufficiently small for collective accretion to become significant. The velocity dispersion of the stars and gas clouds within 30 pc from the Galactic center is $\sigma_G \sim 50 \text{ km s}^{-1}$ (Genzel, Hollenbach & Townes 1994). The central velocity dispersion of pre-collapse cores is typically $\sigma_* \sim 10 \text{ km}$. The fraction of clusters with $C_\infty^2 + u_\infty^2 < \sigma_*^2$ (cf the condition set in equation 15) is $\sim \text{erf}(\sigma_*^2/\sigma_G^2) \sim \sigma_*^2/\sigma_G^2$, which is on the order of a few percent.

For clusters having $M_d \sim 10^4 M_\odot$ and sufficiently small speed relative to the ISM, we find from equation (11) that the gas accretion rate onto the cluster $\dot{M}_c > 10^{23} \text{ gm s}^{-1}$ in regions where the density of the ambient gas near the Galactic center is $> 10^4 \text{ cm}^{-3}$ (Launhardt, Zylka, & Mezger 2002). The accumulation of gas near the center of the cluster potential enables solar-type stars to accrete at a rate $\sim 10^{-6} M_\odot \text{ yr}^{-1}$. Because the accretion rate is proportional to M_*^2 , the growth rate of the stars accelerates rapidly as they accrete mass. That rapid acceleration allows stars with masses of $20 M_\odot$ to be built up within $\sim 1 \text{ Myr}$, by accretion onto stars with initial masses comparable to that of the Sun, a timescale shorter than the lifetimes of the massive stars formed via accretion. With such a small velocity relative to the dense gas, the clusters do not drift more than a few pc from the orbits of any clouds within 1 Myr, which would allow the low-mass mature stars to be rejuvenated into young, massive stars.

The main advantage of this scenario is that it does not require the rapid formation of clusters with unique initial mass functions. In comparison with star forming regions in the Solar neighborhood, the Galactic center is a challenging environment for efficient star formation. Our scenario naturally bypasses the stringent conditions for forming the progenitor clouds in regions where the external tidal effect is strong and heating is intense. This scenario requires a combination of clusters surviving tidal destruction as their orbits decay, and encountering dense gas with sufficiently low relative velocity to lead to significant accretion. Such a combination of events is certainly relatively unlikely. However, in the cold dark matter scenario, the initial population of clusters and dwarf galaxy cores near the center of the Galaxy was much larger than today, such that the population of faint, old clusters near the Galactic center would be significantly larger than predicted from the current population

of globular clusters. A fairly unlikely sequence of events is therefore needed if we are to avoid having many more systems such as the Arches and Quintuplet clusters today.

Additionally, the centers of dense clusters are populated with both white dwarfs and neutron stars (Yanny et al. 1997). Accretion onto these dense stellar cores at the inferred rate can lead to the onset of luminous x-ray sources. Such a process may account for the distinct point sources of X-ray emission found by Chandra in these clusters (Laws & Yusef-Zadeh 2004).

5. Summary and Discussion

In this paper, we examine in detail the accretion of ambient gas by a stellar system. Although the gravitational potential of the individual stars are point mass, that of the cluster is softer. We showed that if either the relative speed of the cluster or the sound speed of the ambient gas is large compared with the velocity dispersion of the core, the accretion by the cluster is inefficient. Individual stars accrete gas as though they move through the interstellar medium independently. But if the relative speed of the cluster and the sound speed of the ambient gas is less than that of the internal velocity dispersion, gas is accreted into the cluster potential collectively and rapidly. Accretion by individual stars is then enhanced greatly relative to their rate of accretion directly from the ambient gas.

We suggest that this process may be important in inducing chemical inhomogeneity and modifying the white dwarf cooling sequence some globular clusters whose orbits happen to lie close to the Galactic plane. We also speculate that this process may have caused some tidally stripped cores of globular clusters near the Galactic center to accrete gas and to rejuvenate their member stars, resulting in the formation of clusters of young, hot stars, such as are seen near the center of the Galaxy.

This work was performed under the auspices of the U.S. Department of Energy by University of California, Lawrence Livermore National Laboratory under Contract W-7405-Eng-48. This work is partially supported by NASA through an astrophysical theory grant NAG5-12151.

REFERENCES

- Andreuzzi, G., Richer, H. B., Limongi, M., & Bolte, M. 2002, *A&A*, 390, 961
- Anninos, P., & Fragile, P. C. 2003, *ApJS*, 144, 243
- Anninos, P., Fragile, P. C., & Murray, S. D. 2003, *ApJS*, 147, 177
- Artymowicz, P., Lin, D. N. C. & Wampler, E. J. 1993, *ApJ*, 409, 592
- Batchelor, G. K. 1967, in *An Introduction to Fluid Dynamics* (Cambridge: Cambridge University Press)
- Binney, J. & Tremaine, S. 1987, in *Galactic Dynamics* (Princeton: Princeton Univ. Press), 30
- Bondi, H. 1952, *MNRAS*, 112, 195
- Cameron, A. G. W., & Fowler, W. A. 1971, *ApJ*, 164, 111
- Castilho, B. V., Pasquini, L., Allen, D. M., Barbuy, B., & Molaro, P. 2000, *A&A*, 361, 92
- Chandrasekhar, S. 1943, *ApJ*, 97, 255
- Chen, L., & Zhao, J. 1999, in *Harmonizing Cosmic Distance Scales in a Post-Hipparcos Era*, eds. D. Egret & A. Heck (San Francisco: ASP), 259
- Cohen, R. L., Guhathakurta, P., Yanny, B., Schneider, D. P., & Bahcall, J. N. 1997, *AJ*, 113, 669
- Deliyannis, C. P., Boesgaard, A. M., & King, J. R. 1995, *ApJ*, 452, L13
- Djorgovski, S. 1993, in *Structure and Dynamics of Globular Clusters*, eds. S. G. Djorgovski & G. Meylan (San Francisco: ASP) 357
- Dong, S., Lin, D. N. C., & Murray, S. D. 2003, *ApJ*, 596, 930
- Fall, S. M., & Rees, M. J. 1985, *MNRAS*, 181, 37P
- Ferraro, F. R., Clementini, G., Fusi Pecci, F., & Buonanno, R. 1991, *MNRAS*, 252, 357
- Ferraro, F. R., Clementini, G., Fusi Pecci, F., Sortino, R., & Buonanno, R. 1992, *MNRAS*, 256, 391
- Figer, D. F., Kim, S. S., Morris, M., Serabyn, E., Rich, R. M., & MacLean, R. S. 1999, *ApJ*, 525, 750

- Figer, D. F. et al. 2002, *ApJ*, 581, 258
- Figer, D. F., Rich, R. M., Kim, S. S., Morris, M., & Serabyn, E. 2004, *ApJ*, 601, 319
- Fragile, P. C., Murray, S. D., Anninos, P., & Lin, D. N. C. 2003, *ApJ*, 590, 778
- Frank, J., King, A., & Raine, D. J. 2002, *Accretion Power in Astrophysics: Third Edition* (Cambridge: Cambridge University Press)
- Geha, M., & Guhathakurta, P., & van der Marel, R. P. 2002, *AJ*, 124, 3073
- Genzel, R., Hollenbach, D., & Townes, C. H. 1994, *Rep. Prog. Phys.*, 57, 417
- Guhathakurta, P., Yanny, B., Schneider, D. P., & Bahcall, J. N. 1996, *AJ*, 111, 267
- Hansen, B. M. S. 1999, *ApJ*, 520, 680
- Hansen, B. M. S., Brewer, J., Fahlman, G. G., Gibson, B. K., Ibata, R., Limongi, M., Rich, R. M., Richer, H. B., Shara, M. M., & Stetson, P. B. 2002, *ApJ*, 574, L155
- Hideaki, M., & Yoshiaki, T. 2003, *ApJ*, 585, 250
- Hoyle, F., & Lyttleton, R. A. 1941, *MNRAS*, 101, 227
- Kalirai, J. S. et al. 2001, *AJ*, 122, 257
- Keenan, D. W. 1979, *A&A*, 71, 245
- Kim, S. S., Figer, D. F., Lee, H. M., & Morris, M. 2000, *ApJ*, 545, 301
- Kim, S. S., & Morris, M. 2003, *ApJ*, 597, 312
- Kim, S. S., Morris, M., & Lee, H. M. 1999, *ApJ*, 525, 228
- Klypin, A., Kravtsov, A. V., Valenzuela, O., & Prada, F. 1999, *ApJ*, 522, 82
- Kraft, R. P., Sneden, C., Langer, G., & Prosser, C. 1992, *AJ*, 104, 645
- Landau, L. D. & Lifshitz, E. M. 1959, in *Fluid Mechanics* (Oxford: Pergamon)
- Langer, G. E., Bolte, M., Prosser, C. F., & Sneden, C. 1992, *BAAS*, 23, 1328
- Laundardt, R., Zylka, R., & Mezger, P. G. 2002, *A&A*, 384, 112
- Laws, C., & Yusef-Zadeh, F. 2004, *ApJ*, in press
- Laws, C., & Gonzalez, G. 2001, *ApJ*, 553, 405

- McMillan, S. L. W., & Portegies Zwart, S. F. 2003, *ApJ*, 596, 314
- Madsen, S., Dravins, D. & Lindegren, L. 2002, *A&A*, 381, 446
- McKee, C. F., & Tan, J. C. 2003, *ApJ*, 585, 850
- Metcalf, R. B. 2002, *ApJ*, 580, 696
- Metcalf, R. B., & Zhao, H. 2002, *ApJ*, 567, L5
- Moore, B., Ghigna, S., Governato, F., Lake, G., Quinn, T., Stadel, J., & Tozzi, P. 1999, *ApJ*, 524, L19
- Murray, S. D., Dong, S., & Lin, D. N. C. 2003, *ApJ*, 593, 301
- Nagata, T., Woodward, C. E., Shure, M., & Kobayashi, N. 1995, *AJ*, 109, 1676
- Nagata, T., Woodward, C. E., Shure, M., & Pipher, J. L. 1990, *ApJ*, 351, 83
- Okuda, H., Shibai, H., Nakagawa, T., Matsuhara, H., Kobayashi, Y., Kaifu, N., Nagata, T., Gatley, I., & Geballe, T. R. 1990, *ApJ*, 351, 89
- Oh, K. S., & Lin, D. N. C. 1992, *ApJ*, 386, 519
- Oh, K. S., Lin, D. N. C., & Aarseth, S. 1995, *ApJ*, 442, 142
- Ostriker, J. P. & Gnedin, O. Y. 1997, *MNRAS*, 487, 667
- Penny, A. J. & Dickens, R. J. 1986, *MNRAS*, 220, 845
- Perryman, M. A. C., Brown, A. G. A., Lebreton, Y., Gomez, Z., Turon, C., de Strobel, C., Cayrel, R., Mermilliod J. C., Robichon, N., Kovalevsky, J., & Crifo, F. 1998, *A&A*, 331, 81
- Peterson, R., & Caldwell, N. 1993, *AJ*, 105, 1411
- Plummer, H. C. 1911, *MNRAS*, 71, 460
- Portegies Zwart, S. F., McMillan, S. L. W., & Gerhard, O. 2003, *ApJ*, 593, 352
- Pryor, C., & Meylan, G. 1993, in *Structure and Dynamics of Globular Clusters*, eds. S. G. Djorgovski & G. Meylan (San Francisco: ASP) 357
- Quillen, A. C. 2002, *ApJ*, 124, 400
- Richer, H. B., & Fahlman, G. G. 1986, *ApJ*, 381, 147

- Richer, H. B., Fahlman, G. G., Rosvick, J., & Ibata, R. 1998, *ApJ*, 504, L91
- Richer, H. B., Fahlman, G. G., Ibata, R. A., Pryor, C., Bell, R. A., Bolte, M., Bond, H. E., Harris, W. E., Hesser, J. E., Holland, S., Ivanan, N., Mandushev, G., Stetson, P. B., & Wood, M. A. 1997, *ApJ*, 484, 741
- Sackman, I.-J., & Boothroyd, A. I. 1992, *ApJ*, 392, L71
- Sackman, I.-J., Smith, R. L., & Despain, K. H. 1974, *ApJ*, 187, 555
- Sandquist, E. L., Dokter, J. J., Lin, D. N. C., & Mardling, R. A. 2002, *ApJ*, 572, 1012
- Shu, F. H. 1992, in *The Physics of Astrophysics Vol. II: Gas Dynamics*, (Mill Valley: University Science Books), 77
- Stetson, P. B., & Harris, W. E. 1988, *AJ*, 96, 909
- Stolte, A., Grebel, E. K., Brandner, W. & Figer, D. F. 2002, *A&A*, 394, 459
- Suntzeff, N. 1993, in *The Globular Cluster-Galaxy Connection*, eds. G. H. Smith & J. P. Brodie (San Francisco: ASP), 167
- van den Bosch, F. C., Lewis, G. F., Lake, G., & Stadel, J. 1999, *ApJ*, 515, 50
- Vesperini, E. 1998, *MNRAS*, 299, 1019
- von Hippel, T., & Gilmore, G. 2000, *AJ*, 120, 1384
- Wilden, B. S., Jones, B. F., Lin, D. N. C., & Soderblom, D. R. 2002, *AJ*, 124, 2799
- Yanny, B., Guhathakurta, P., Schneider, D. P. & Bahcall, J. N. 1994, *ApJ*, 435, L59

Table 1. Models

Model	V km s ⁻¹	c_s km s ⁻¹	R_B pc	τ_c Myr	τ_s Myr	M_p M _⊙	M_{acc} M _⊙
1	30	1	1.7	3.8	1.65	2.4×10 ⁴	3.4×10 ¹
2	10	1	14.8	11.4	14.6	2.0×10 ⁶	6.0×10 ⁶
3	1	1	740	114	730	4.9×10 ⁹	2.2×10 ⁷
4	10	10	7.4	11.4	0.73	4.9×10 ³	2.1×10 ⁴
5	1	10	14.8	114	1.46	2.0×10 ⁴	3.2×10 ⁴
6	1	30	1.6	114	0.054	2.4×10 ¹	3.4×10 ³

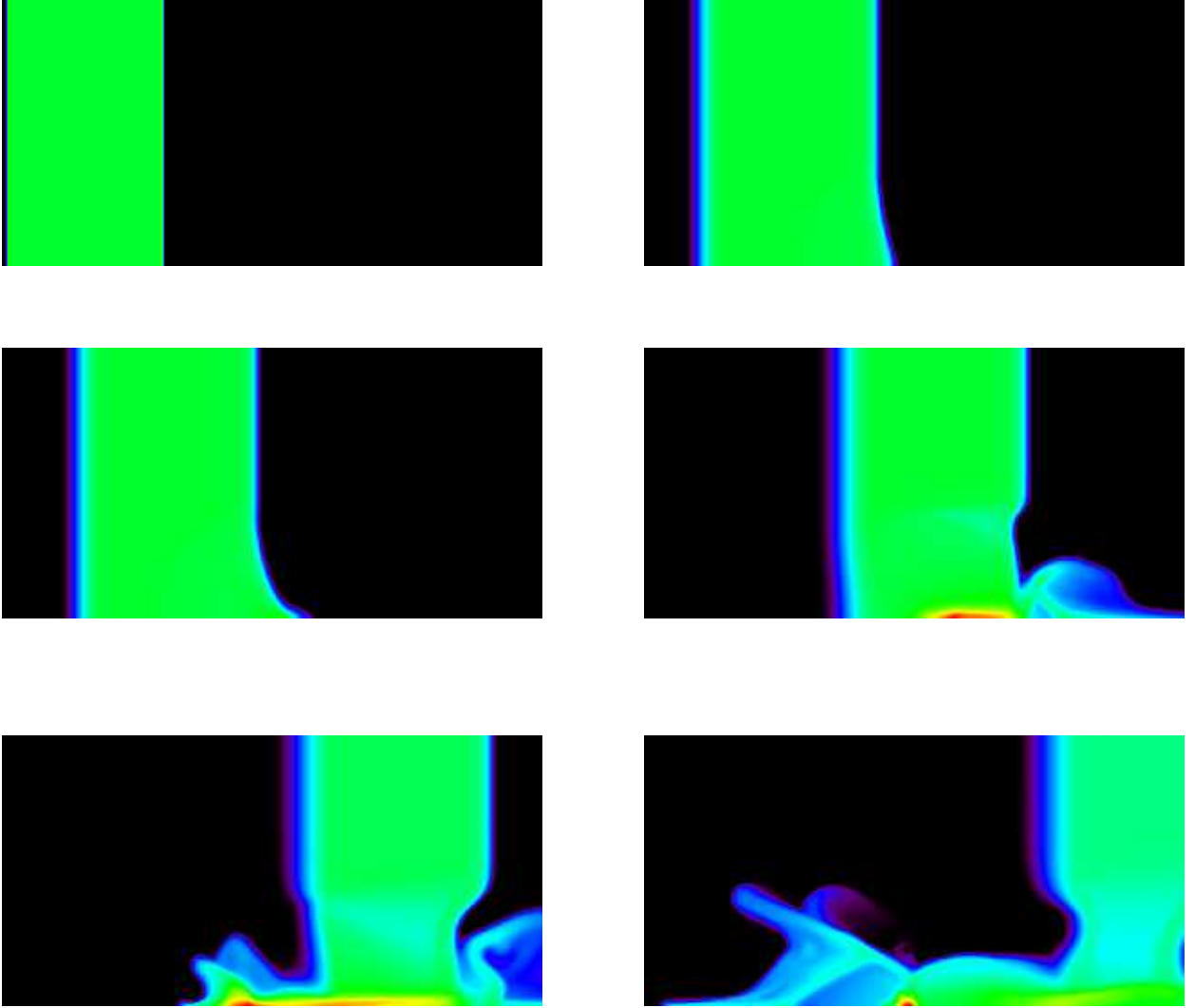


Fig. 1.— The density evolution of Model 2. The model is shown at the times 0, 4.5, 6.0, 7.5, 22.5, and 30 Myr. The dense cloud, modelled as a simple slab of gas, sweeps from left to right across the accreting potential, centered in the model. Because of the relatively deep potential, and slow speed relative to the cloud, the potential has a significant effect upon the dense gas. Some of the gas is initially pulled ahead of the rest of the cloud into the potential, and much of the gas within the tidal radius is accreted as the cloud passes by the potential, where it forms the small, dense core seen in the final frame.